

Analysis of the Phase-Shifted Carrier Modulation for Modular Multilevel Converters

¹ M Aparna, ² C. Ashok Kumar

¹PG Student, Department of Electrical and Electronics Engineering, Sai Rajeswari Institute of Technology, Kadapa, Andhra Pradesh, India

²Assistant Professor, Department of Electrical and Electronics Engineering, Sai Rajeswari Institute of Technology, Kadapa, Andhra Pradesh, India

ABSTRACT

The Modular multilevel converter (MMC) is a rising topology for high-Power applications and is considered as the improvement pattern of the high-voltage power converters. In this paper, general implementation of the phase-shifted carrier (PSC) modulation with a capacitor voltage balancing method for MMC is first presented. At that point, the numerical investigation of PSC modulation for MMC is performed to distinguish the PWM harmonic characteristics of the output voltage and the circulating current. Additionally, impact of the carrier displacement angle between the upper and lower arms on these harmonics is likewise examined. Utilizing this Analysis, the optimum displacement angels are indicated for the output voltage harmonics minimization and the circulating current harmonic cancellation, respectively. The symphonious elements of the line-to-line voltage and the dc-link current are additionally researched. In addition, an expansion of the PSC regulation for MMC with full-connect submodules is likewise proposed which can build the identical switching frequency of the output voltage and circulating current by two times contrasted and the customary MMC.

Keywords : Fourier series, modular multilevel converter (MMC), phase-shifted carrier (PSC), pulse width modulation (PWM).

I. INTRODUCTION

These days, the expanding concerns about environmental change and the developing interest for electricity have postured new difficulties for power generation and transmission [1]–[3]. As an imaginative and exceptionally effective answer for energy conversion, the measured multilevel converter (MMC) is increasing an ever increasing number of considerations since it Presents extraordinary points of interest contrasted and customary two-level or three-level voltage source converters.

These focal points, for example, lower losses, diminished EMI noise, less semiconductor device stress, adaptability and simple assembling, and the about perfect sinusoidal-modulated output waveforms make MMC the most appealing topology for high-voltage high-power applications, especially in the high-voltage direct current transmission (HVDC) sector [4]–[8]. Numerous acadamic papers have been distributed to enhance the exhibitions of MMC. In [9]–[16], the numerical investigation, modeling methodologies, and the semiconductor prerequisites of MMC under various working conditions were done. The capacitor voltage balancing and circulating current suppression are two

noteworthy assignments related with MMC and a few control arrangements in light of feedback control or the sorting algorithm have been proposed and detailed in [17]. What's more, as a standout amongst the most fascinating themes, different pulse width modulation (PWM) techniques have been produced to fit MMC. The Nearest level control (NLC), otherwise called the round technique, was received in [11],, and. This technique is particularly appropriate for MMC with a substantial number of sub modules (SMs). Besides, [16] and broaden the application extent of NLC by presenting one SM working in PWM operation.

A phase disposition (PD) level shifted PWM system including a voltage balancing technique was examined. Especially, it must be brought up that the PD-PWM is not exceptionally favored for MMC, as it causes an uneven power dissemination among the distinctive SMs. Another prevalent PWM strategy is the Phase shifted carrier (PSC), which is the most usually utilized technique in the cascaded H-bridge converters (CHB). The PSC balance is additionally appealing to MMC as it has some particular elements:

1) The semiconductor stress and the power handled care of by every SM are equitably dispersed. Subsequently, the capacitor voltage balancing control can be effortlessly accomplished.

2) The output voltage has a high resulting about switching frequency and a low total harmonic distortion (THD).

3) Consistent with the structure of MMC, each triangular carrier related to a specific SM exhibits the idea of nature of modularity and scalability

Due to the previously mentioned merits, the PSC scheme of CHB has been straightforwardly utilized to MMC by numerous scientists in [18], that the carrier for SMs in a similar phase are arrange with an equivalent phase moves in angle. There are, be that as it may, noteworthy contrasts between these two

topologies. For the instance of the CHB, countless dc sources are required while exchanging active power, which must be sustained from phase shifting transformers and multiphase rectifiers, which are extremely costly and bulky. Conversely, MMC takes out the bulky phase moving transformers and has an extra dc terminal shaped by the upper and lower arms, which permits bi-directional power flow amongst ac and dc sides. Also, the output voltage and circulating current of MMC are dictated by the associations between the upper and the lower arm voltages [9]. Thus, while applying PSC modulation to MMC, transporters for SMs in the lower arm and carrier for SMs in the upper arm should be considered independently, with an interleaved displacement angle. This displacement angle will influence the high-frequency interactions between the upper and lower arms, and further decides the harmonic components of MMC.

Up until this point, few analysis have investigated the standard of PSC modulation for MMC and it stays vague how the displacement angle would impact the execution of MMC. It is, along these lines, the point of this paper to give a completely scientific analysis of the PSC modulation executed in MMC, to research the effect of the displacement angle on the voltage and current harmonics, and to discover an ideal dislodging angle which can limit these harmonics.

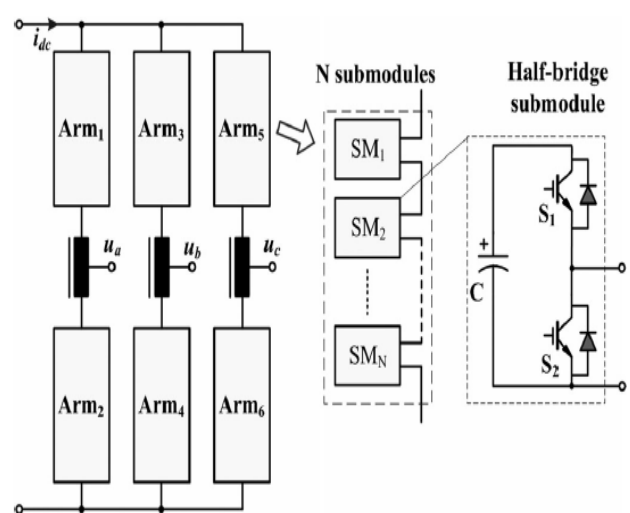


Fig. 1. Circuit configuration of the MMC.

II. BASIC OPERATING PRINCIPLES

A. Structure of MMC

The circuit design of a three-phase MMC is appeared in Fig. 1. Each period of MMC comprises of two arms, the upper and the lower, which are associated through buffer inductors. Each arm is framed by an arrangement association of N nominally indistinguishable half-connect SMs and every SM contains a dc capacitor and two insulated gate bipolar transistors (IGBTs). The single coupled inductor is favored in this paper as it has small size and lighter weight than the total of the two separate inductors [5].

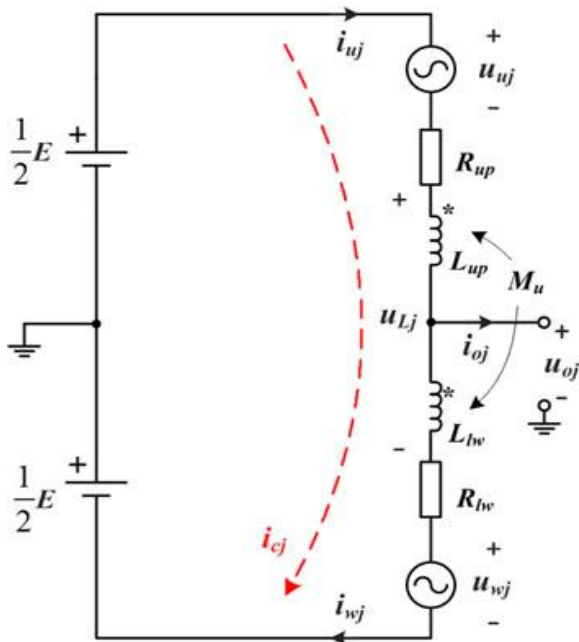


Fig. 2. Equivalent circuit of one phase of the MMC

B. Mathematical Model of MMC

As appeared in Fig. 2, the equivalent circuit diagram of one period of MMC is utilized for analysis. u_{oj} is the output voltage of phase ($j \in \{a, b, c\}$), i_{oj} is the phase current, and E is the dc-link voltage. u_{uj} , i_{uj} , and u_{wj} , i_{wj} represent to the voltages and streams of the upper arm and the lower arm, individually.

The following equations can be obtained by Kirchhoff's voltage law:

$$R_{up}i_{uj} + L_{up}\frac{di_{uj}}{dt} + M_u\frac{di_{wj}}{dt} = \frac{E}{2} - u_{uj} - u_{oj} \quad (1)$$

$$R_{lw}i_{wj} + L_{lw}\frac{di_{wj}}{dt} + M_u\frac{di_{uj}}{dt} = \frac{E}{2} - u_{wj} + u_{oj} \quad (2)$$

$$u_{Lj} = L_{up}\frac{di_{uj}}{dt} + M_u\frac{di_{wj}}{dt} + L_{lw}\frac{di_{wj}}{dt} + M_u\frac{di_{uj}}{dt} \quad (3)$$

where u_{Lj} is the voltage across the coupled inductors, M_u is the common inductance, R_{up} , R_{lw} and L_{up} , L_{lw} are simply the resistances and self inductances, respectively. It is accepted that the coupling coefficient of two windings equals with 1 (i.e., $p = L_{lw} = M_u = L_0$) and the resistances of the inductors are ignored for effortlessness. Consequently, the articulations (1)–(3) can be inferred as

$$u_{oj} = \frac{1}{2}(u_{wj} - u_{uj}) \quad (4)$$

$$u_{Lj} = -u_{wj} - u_{uj} + E = 4L_0\frac{di_{cj}}{dt} \quad (5)$$

where i_{cj} is defined as the circulating current of phase j , which circulates through both the upper and lower arms and can be given by

$$i_{cj} = \frac{1}{2}(i_{uj} + i_{wj}). \quad (6)$$

According to (5), the circulating current i_{cj} can be obtained by performing the following integration:

$$i_{cj} = I_{cj} + \int_0^t \frac{u_{Lj}}{4L_0} dt \quad (7)$$

where I_{cj} is the dc component of the circulating current. Ideally, the phase current i_{oj} would be split equally between these two arms and the arm currents can be expressed as

$$i_{uj} = i_{cj} + \frac{1}{2}i_{oj} \quad (8)$$

$$i_{wj} = i_{cj} - \frac{1}{2}i_{oj}. \quad (9)$$

III. IMPLEMENTATION OF PSC MODULATION INTO MMCS

A. Description of the PSC Modulation for MMC

As portrayed in Fig. 3, while applying the PSC modulation to a MMC with N SMs per arm, there ought to be a sum of 2 N triangular carriers with the frequency of f_c ($C_{u1} - C_{uN}$ for the upper arm, and $C_{l1} - C_{lN}$ for the lower arm) and 2 N reference signals ($u_{ref_{uj}}(i)$ for the i^{th} SM in the upper arm, and $u_{ref_{lj}}(i)$ for the i^{th} SM in the lower arm, $i=1, 2, \dots, N$). Every SM is allocated with a particular reference signal and a triangular carrier, to such an extent that all SMs have a similar switching frequency and the semiconductor stresses are equally circulated. At that point, the switching pulses of every SM are created by contrasting the reference signal and the relating carrier wave.

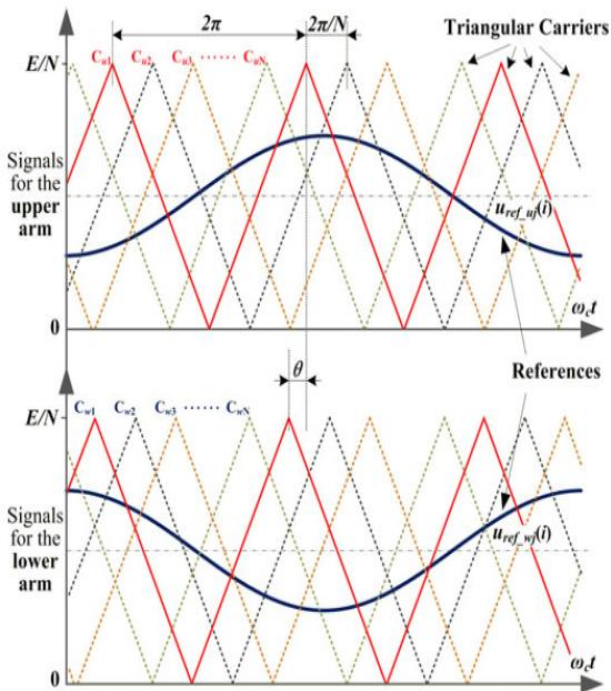


Fig. 3. PSC-PWM of MMC.

In order to achieve best harmonic cancellation features, then triangular carriers of each arm are shifted by $2\pi/N$ incrementally. Therefore, the phase angle $\theta_w(i)$ of the i^{th} carrier C_{wj} in the lower arm can be given by

$$\theta_w(i) = \frac{2\pi}{N} \times (i - 1). \quad (10)$$

As for the i^{th} carrier C_{uj} in the upper arm, that is

$$\theta_u(i) = \theta + \frac{2\pi}{N} \times (i - 1). \quad (11)$$

where θ is characterized as the removal point between the upper and lower bearers. Note that θ significantly affects the harmonic components of MMC and will be talked about in Section IV. Because of symmetry, the scope of θ can be gotten as $[0, \pi/N]$.

B. Capacitor Voltage Balancing Method

As the SMs of MMC are modulated independently under PSC-PWM, the voltage balancing of the capacitors can be achieved by balancing the reference signal of each SM. Fig. 4 shows the complete block diagram of PSC-PWM for MMC combined with the capacitor voltage balancing method, in which the reference signals $u_{ref_{wj}}(i)$ and $u_{ref_{uj}}(i)$ are given by

$$u_{ref_{uj}}(i) = \frac{E}{2N} (1 + M \cos(\omega_0 t + \varphi_j)) + \Delta u_{ref_{uj}}(i) \quad (12)$$

$$u_{ref_{lj}}(i) = \frac{E}{2N} (1 + M \cos(\omega_0 t + \varphi_j + \pi)) + \Delta u_{ref_{lj}}(i) \quad (13)$$

where M ($0 \leq M \leq 1$) denotes the modulation depth, ω_0 is the angular frequency of the output ac voltage, and φ_j is the phase angle. $\Delta u_{ref_{wj}}(i)$ and $\Delta u_{ref_{uj}}(i)$ represent the reference adjustment of each SM in the lower and the upper arm, respectively. These reference adjustments are intended for the voltage balancing control of the SMs and can be calculated as

$$\Delta u_{ref_{uj}}(i) = K_p (U_{avg_j} - U_{SM_uj}(i)) \times i_{cj} \quad (14)$$

$$\Delta u_{ref_{lj}}(i) = K_p (U_{avg_j} - U_{SM_lj}(i)) \times i_{cj} \quad (15)$$

where K_p signifies the corresponding addition, $U_{SM_uj}(i)$ is the capacitor voltage of i^{th} SM in the lower arm, while $U_{SM_lj}(i)$ is the capacitor voltage of i^{th} SM in the upper arm. u_{avg_j} is the normal voltage of all the $2N$ SM capacitors inside phase j . Conditions

(14) and (15) show that for the SMs with voltages lower than the average voltage, the result of the change voltage and the circulating current i_{cj} will frame a positive power transferred to charge these SMs. Conversely, a negative power transfer will be produced to release the SMs with voltages higher than the normal voltage. Detailed implementation usage of the proposed voltage balancing control strategy can be found in Fig. 4.

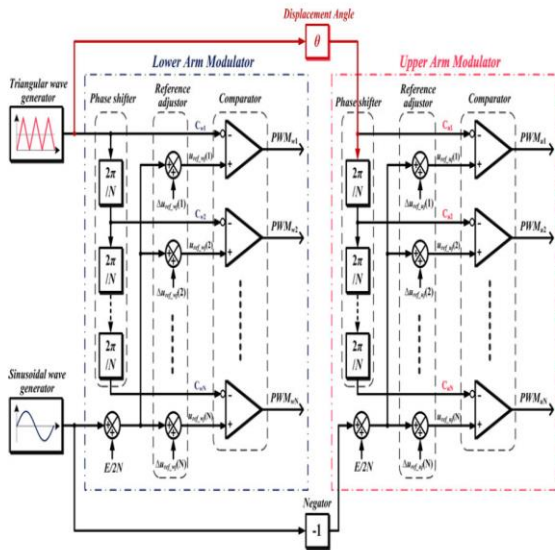


Fig. 4. Block diagram of the PSC-PWM applied to an MMC.

IV. HARMONIC FEATURES OF MMC WITH PSC MODULATION

In this section, the double Fourier series based analysis is exhibited to explore how the displacement angle of PSC modulation will impact the harmonics of the output phase voltage and the circulating current of MMC. In addition, the optimum displacement angles to limit the voltage harmonics and to wipe out the flowing current sounds are additionally proposed, respectively.

A. Influence of the Displacement Angle on Harmonics of Output Voltage and Circulating Current of MMC

In the following harmonic analysis, it is assumed that all the capacitor voltages are naturally balanced (i.e., $\Delta u_{ref_{wj}}(i) = \Delta u_{ref_{uj}}(i) = 0$) thus the dc-link voltage

E is equally distributed among the SMs (i.e., $USM = E/N$). Note that this assumption is reasonable because $\Delta u_{ref_{wj}}(i)$ and $\Delta u_{ref_{uj}}(i)$ are generally a relatively small portion when compared with $u_{ref_{wj}}(i)$ and $u_{ref_{uj}}(i)$, which can be proved by the experimental results in Section VI. Moreover, in normal operating conditions, the capacitance of each SM is always designed to limit the capacitor voltage fluctuations not exceeding 10% of the rated capacitor voltage. So for simplicity, the capacitance of each SM is supposed to be large enough so that the capacitor voltage fluctuations can be ignored. According to (12), the Fourier representation of the output voltage of i^{th} SM in the lower arm, $u_{ref}(i)$, can be expressed as

$$u_{wj}(i) = \frac{E}{2N} + \frac{ME}{2N} \cos(\omega_o t + \varphi_j) + \sum_{m=1}^{\infty} \sum_{n=-\infty}^{\infty} \frac{2E}{m\pi N} \times \sin\left[\frac{(m+n)\pi}{2}\right] \times J_n\left(\frac{Mm\pi}{2}\right) \times \cos\left[m\left(\omega_c t + (i-1)\frac{2\pi}{N}\right) + n(\omega_o t + \varphi_j)\right] \quad (16)$$

where ω_c is the angular frequency of the triangular carriers, m is the harmonic order of the carrier wave ($m = 1, \dots, \infty$), n is the harmonic order of the reference wave ($n = -\infty, \dots, -1, 0, 1, \dots, \infty$), $J_n(x)$ refers to the Bessel coefficient of order n and argument x .

From (13), the output voltage of i^{th} SM in the upper arm, $u_{uj}(i)$, can also be described by the same way

$$u_{uj}(i) = \frac{E}{2N} - \frac{ME}{2N} \cos(\omega_o t + \varphi_j) + \sum_{m=1}^{\infty} \sum_{n=-\infty}^{\infty} \frac{2E}{m\pi N} \times \sin\left[\frac{(m+n)\pi}{2}\right] \times J_n\left(\frac{Mm\pi}{2}\right) \times \cos\left[m\left(\omega_c t + \theta + (i-1)\frac{2\pi}{N}\right) + n(\omega_o t + \varphi_j + \pi)\right]. \quad (17)$$

By summing the output voltages of N SMs, the arm voltages can be derived as

$$u_{wj} = \sum_{i=1}^N u_{wj}(i) = \frac{E}{2} + \frac{ME}{2} \cos(\omega_o t + \varphi_j) + \sum_{m=1}^{\infty} \sum_{n=-\infty}^{\infty} \frac{2E}{m\pi N} \sin\left[\frac{(Nm+n)\pi}{2}\right] \times J_n\left(\frac{MNm\pi}{2}\right) \cos[Nm\omega_c t + n(\omega_o t + \varphi_j)] \quad (18)$$

$$u_{uj} = \sum_{i=1}^N u_{uj}(i) = \frac{E}{2} - \frac{ME}{2} \cos(\omega_o t + \varphi_j) + \sum_{m=1}^{\infty} \sum_{n=-\infty}^{\infty} \frac{2E}{m\pi N} \sin\left[\frac{(Nm+n)\pi}{2}\right] \times J_n\left(\frac{MNm\pi}{2}\right) \cos[Nm(\omega_c t + \theta) + n(\omega_o t + \varphi_j + \pi)]. \quad (19)$$

Equations (18) and (19) show that all harmonics are eliminated except those at N-multiples of the carrier frequency and their sideband components. Combining (4), (5), and (7) with (18) and (19), the output voltage and the circulating current of phase j can be obtained as (see Appendix A)

$$u_{oj} = \frac{1}{2}ME \cos(\omega_o t + \varphi_j) + \sum_{m=1}^{\infty} \sum_{n=-\infty}^{\infty} \frac{(-1)^n 2E}{m\pi N} \times J_{2n+1-Nm}\left(\frac{MNm\pi}{2}\right) \times \cos[Nm\omega_c t + Q] \cos\left[\frac{Nm(\theta - \pi)}{2}\right] \quad (20)$$

$$i_{cj} = \frac{I_{dc}}{3} - \sum_{m=1}^{\infty} \sum_{n=-\infty}^{\infty} \frac{(-1)^n E \times J_{2n+1-Nm}(MNm\pi/2)}{m\pi N L_0 (Nm\omega_c + (2n+1-Nm)\omega_o)} \times \cos[Nm\omega_c t + Q] \sin\left[\frac{Nm(\theta - \pi)}{2}\right] \quad (21)$$

Where

$$Q = (2n+1-Nm)(\omega_o t + \varphi_j) + \frac{Nm(\theta - \pi)}{2}. \quad (22)$$

It can be seen that the phase voltage u_{oj} and the circulating current i_{cj} both contain N-multiples of the carrier frequency harmonics with associated sideband components. Note that (21) focuses on the switching harmonics caused by PSC-PWM whereas not includes the low-frequency harmonics due to the energy oscillation between the upper and lower arms [9]. To analyze the impact of the displacement angle θ

on the harmonic features, magnitudes of the Nm^{th} carrier group harmonics of u_{oj} and i_{cj} are defined as \hat{V}_{mn} and \hat{I}_{mn} respectively.

Therefore

$$\hat{V}_{mn} = K_{mn} \times \left| \cos\left[\frac{Nm(\theta - \pi)}{2}\right] \right| \quad (23)$$

$$\hat{I}_{mn} = H_{mn} \times \left| \sin\left[\frac{Nm(\theta - \pi)}{2}\right] \right| \quad (24)$$

Where

$$K_{mn} = \frac{2E}{m\pi N} \left| J_{2n+1-Nm}\left(\frac{MNm\pi}{2}\right) \right| \quad (25)$$

$$H_{mn} = \frac{K_{mn}}{2L_0 (Nm\omega_c + (2n+1-Nm)\omega_o)}. \quad (26)$$

Figs. 5 and 6 demonstrate the extents of the Nm^{th} carrier group harmonics of the output voltage and the circulating current as a component of displacement angle θ , respectively. Here, just the initial six harmonic groups ($m \leq 6$) are investigated because of the impediment of this paper. It can be seen that for a specific harmonic group m , the voltage harmonic and the current harmonic are changed with θ at direct inverse propensity. It implies that a base voltage harmonic is gotten at the cost of a maximum circulating current harmonics, and the other way around. In this way, the displacement angle θ ought to be outlined particularly as indicated by the prerequisites of use conditions.

B. Output Voltage Harmonics Minimization PSC Scheme

For most power converters, the output voltage with a higher resulting switching frequency and a lower harmonic mutilation implies littler and lower cost filters. In this way, from (23) and Fig. 5, the base voltage harmonics can be acquired in MMC by choosing the displacement angle as follows:

$$\theta = \begin{cases} 0, & N \text{ is odd} \\ \frac{\pi}{N}, & N \text{ is even} \end{cases} \quad (27)$$

Then, the phase output voltage can be derived as

$$u_{oj} = \frac{1}{2}ME \cos(\omega_o t + \varphi_j) + \sum_{m=1}^{\infty} \sum_{n=-\infty}^{\infty} \frac{(-1)^{n+1} E}{m\pi N} \\ \times J_{2n+1-2Nm} (MNm\pi) \cos [2Nm\omega_c t + Q'] \quad (28)$$

Where Q' is given by

$$Q' = (2n + 1 - 2Nm) (\omega_o t + \varphi_j). \quad (29)$$

Clearly, voltage harmonics at odd products of the Nm^{th} carrier group will be zero and the frequency of the most reduced harmonic group ascends to $2Nf_c$. In this manner, the cutoff frequency of the output filter can be multiplied, prompting a noteworthy decrease of the filter measure. With respect to the flowing current at this dislodging point, even products of the Nm^{th} carrier group harmonics are crossed out while odd products will achieve their greatest esteems

$$\hat{I}_{mn} = H_{mn}, \quad m = 1, 3, 5, \dots \quad (30)$$

Note that these present sounds won't just motivation a lower productivity of MMC, yet apply a higher current worry upon the semiconductors. In addition, if a smooth dc current is fancied, additional filter must be added to the dc interface so as to lessen these present harmonics.

C. Circulating Current Harmonics Cancellation PSC Scheme

For MMC with an extraordinary number of SMs (e.g., in the HVDC application, N dependably rises to a few hundred), the THD of the output voltage itself will be greatly low and even no air conditioner filters are required. Subsequently, the harmonics of the circulating current turn into the fundamental issue, which ought to be controlled at littler sizes to lessen misfortune and the present anxiety. From (24) and Fig. 6, all the exchanging

sounds of the circulating current can be totally disposed of with the accompanying dislodging angle:

$$\theta = \begin{cases} \frac{\pi}{N}, & N \text{ is odd} \\ 0, & N \text{ is even} \end{cases} \quad (31)$$

Under this condition, an immaculate flowing current can be accomplished without undesirable exchanging sounds subsequently the dc filters are a bit much any longer. In the mean time, with this dislodging angle, the voltage sounds are maximums

$$\hat{V}_{mn} = K_{mn}. \quad (32)$$

D. Harmonic Features of the Line-to-Line Voltage and DC-Link Current of MMC with PSC Modulation

For a three-phase MMC system, the reference signals of phase j ($j \in \{a, b, c\}$) can be obtained according to (12) and (13), where the phase angle is given by

$$\varphi_a = 0, \varphi_b = -\frac{2\pi}{3}, \varphi_c = +\frac{2\pi}{3}. \quad (33)$$

From (20), the line-to-line output voltage can be calculated, that is

$$u_{ab} = u_{oa} - u_{ob} = \frac{\sqrt{3}}{2}ME \cos \left(\omega_o t + \frac{\pi}{6} \right) \\ + \sum_{m=1}^{\infty} \sum_{n=-\infty}^{\infty} \frac{(-1)^n 4E}{m\pi N} \sin [Nm\omega_c t + Q''] \\ \times J_{2n+1-Nm} \left(\frac{MNm\pi}{2} \right) \cos \left[\frac{Nm(\theta - \pi)}{2} \right] \\ \times \sin \left[\frac{(2n + 1 - Nm)\pi}{3} \right] \quad (34)$$

Where

$$Q'' = (2n + 1 - Nm)\omega_o t + \frac{3Nm\theta - Nm\pi}{6} + \frac{(2n + 1)\pi}{3}. \quad (35)$$

In this case, all the triplen sideband harmonics of u_{ab} are cancelled (i.e., $2n + 1 \cdot Nm = 3, 6, 9, \dots$) as the term of "sin $[(2n + 1 \cdot Nm)\delta/3]$ " in (34) is always zero.

Based on (23), the line-to-line voltage magnitudes of the Nm^{th} carrier group harmonics can be expressed as

$$\hat{V}_{ll,mn} = \begin{cases} \sqrt{3}K_{mn} \left| \cos \left[\frac{Nm(\theta-\pi)}{2} \right] \right|, & \text{if } 2n+1-Nm \neq 0, 3, 6, \dots \\ 0, & \text{else.} \end{cases} \quad (36)$$

Similarly, according to (21), the total dc-link current I_{dc} can also be obtained by summing the three phase circulating currents as

$$\begin{aligned} i_{dc} &= \sum_{j=a,b,c} i_{cj} = I_{dc} \\ &= - \sum_{m=1}^{\infty} \sum_{n=-\infty}^{\infty} \frac{(-1)^n E \times J_{2n+1-Nm} \left(\frac{MNm\pi}{2} \right)}{m\pi N L_0 (Nm\omega_c + (2n+1-Nm)\omega_o)} \\ &\quad \times \cos [Nm\omega_c t + Q] \times \sin \left[\frac{Nm(\theta-\pi)}{2} \right] \\ &\quad \times \left\{ 2\cos \left[\frac{(2n+1-Nm)2\pi}{3} \right] + 1 \right\}. \end{aligned} \quad (37)$$

Contrary with the line-to-line voltage, all the sideband harmonics of the dc-link current are eliminated except those at triplen frequency. From (24), the magnitude of the Nm^{th} carrier group harmonics of the dc-link current can be obtained as

$$\hat{I}_{dc,mn} = \begin{cases} 3H_{mn} \left| \sin \left[\frac{Nm(\theta-\pi)}{2} \right] \right|, & \text{if } 2n+1-Nm = 0, 3, 6, \dots \\ 0, & \text{else.} \end{cases} \quad (38)$$

Note that (36) and (38) are still a function of displacement angle δ , the output voltage harmonics minimization and circulating current harmonics cancellation scheme as indicated above are also valid for the line-to-line voltage and dc-link current.

V. PSC MODULATION FOR MMC WITH FULL-BRIDGE SMS

Fig. 7 demonstrates another SM setup of MMC, the full extension structure [5], [6]. In spite of the fact that it needs twofold the quantity of semiconductors contrasted with half-connect MMC, the full-connect MMC can switch the extremity of the dc-interface

voltage and can remove the dc-side short out current effectively by killing all the IGBTs. As it were, full-connect MMC can ensure against dc arrange deficiencies, which is an amazing trademark particularly in HVDC applications. Also, the full-connect MMC can give a supported air conditioning voltage which is higher than the dc-interface voltage. It is, in this manner, likewise an exceptionally appealing topology for sustainable power era applications.

where the dc-connect voltage may shift in a wide range. In this area, an expansion of the PSC regulation for MMC with full-connect SMs is performed, and the ideal relocation point to limit the output voltage harmonics or to dispose of the flowing current is likewise found, individually.

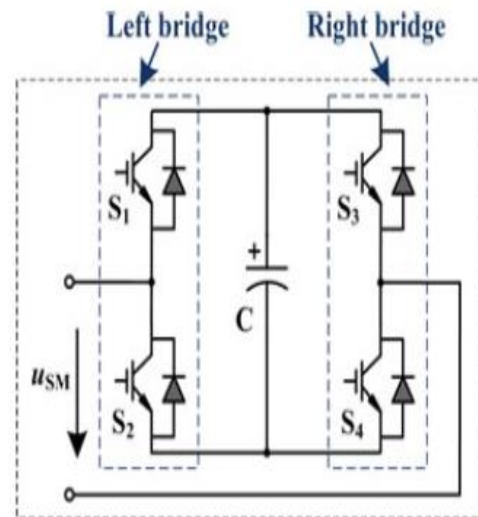


Fig. 7. Configuration of a full-bridge SM.

A. PSC for Full-Bridge MMC

As shown in Fig. 8, the proposed PSC-PWM scheme of the full-bridge MMC is basically the same as that of Fig. 3 except for the following two modifications. One is that the carriers in each arm are shifted by δ/N and the range of the displacement angle δ is now changed to

$$0 \leq \theta \leq \frac{\pi}{2N}. \quad (39)$$

The other modification is that there are two reference signals for each SM, one for the left bridge and the

other for the right bridge. With respect to the i th SM in the lower arm, these references is given by

$$\begin{cases} u_{\text{ref}_-u_j_left}(i) = \frac{3E}{4N} + \frac{ME}{4N} \cos(\omega_o t + \varphi_j) + \Delta u_{\text{ref}_-u_j}(i) \\ u_{\text{ref}_-u_j_right}(i) \\ = \frac{E}{4N} + \frac{ME}{4N} \cos(\omega_o t + \varphi_j + \pi) - \Delta u_{\text{ref}_-u_j}(i) \end{cases} \quad (40)$$

Similarly, for the i th SM in the upper arm , that is

$$\begin{cases} u_{\text{ref}_-u_j_left}(i) = \frac{3E}{4N} + \frac{ME}{4N} \cos(\omega_o t + \varphi_j + \pi) + \Delta u_{\text{ref}_-u_j}(i) \\ u_{\text{ref}_-u_j_right}(i) = \frac{E}{4N} + \frac{ME}{4N} \cos(\omega_o t + \varphi_j) - \Delta u_{\text{ref}_-u_j}(i) \end{cases} \quad (41)$$

Note that the capacitor voltage balancing method proposed in Section III for half-bridge MMCs is also effective for full bridge MMCs and the reference adjustments $\Delta u_{\text{ref}_-u_j}(i)$ and $\Delta u_{\text{ref}_-u_j}(i)$ can still be obtained from (14) and (15). Thus, the output voltage and circulating current of phase j can be obtained as

$$\begin{aligned} u_{oj} &= \frac{1}{2}ME \cos(\omega_o t + \varphi_j) + \sum_{m=1}^{\infty} \sum_{n=-\infty}^{\infty} \frac{(-1)^{N_m+n} 2E}{m\pi N} \\ &\times J_{2n+1-N_m} \left(\frac{MNm\pi}{2} \right) \\ &\times \cos[2Nm\omega_c t + Q'''] \cos \left[Nm \left(\theta - \frac{\pi}{2} \right) \right] \end{aligned} \quad (42)$$

$$\begin{aligned} i_{cj} &= \frac{I_{dc}}{3} \\ &- \sum_{m=1}^{\infty} \sum_{n=-\infty}^{\infty} \frac{(-1)^{N_m+n} E \times J_{2n+1-N_m} (MNm\pi/2)}{m\pi N L_0 (2Nm\omega_c + (2n+1-N_m)\omega_o)} \\ &\times \sin[2Nm\omega_c t + Q'''] \sin \left[Nm \left(\theta - \frac{\pi}{2} \right) \right] \end{aligned} \quad (43)$$

Where

$$Q''' = (2n+1-N_m)(\omega_o t + \varphi_j) + Nm \left(\theta - \frac{\pi}{2} \right). \quad (44)$$

Comparing (42) and (43) to (20) and (21), it can be perceived that full-bridge MMC can double the frequency of the harmonics of the output voltage as well as the circulating current, which means a much smaller filter can satisfy the same THD requirements.

B. Output Voltage Harmonics Minimization PSC Scheme

Similar with the derivation of (27), the output voltage harmonics minimization PSC scheme for full-bridge MMC is also valid by revising the displacement angle as

$$\theta = \begin{cases} 0, & N \text{ is odd} \\ \frac{\pi}{2N}, & N \text{ is even} \end{cases} \quad (45)$$

In this way, the lowest harmonic frequency of the output voltage can increase to $4Nf_c$.

C. Circulating Current Harmonics Cancellation PSC Scheme

For full-bridge MMC, all the switching harmonics of the circulating current can also be eliminated when the displacement angle is selected as

$$\theta = \begin{cases} \frac{\pi}{2N}, & N \text{ is odd} \\ 0, & N \text{ is even} \end{cases} \quad (46)$$

D. Comparison Between the Proposed PSC for Full-Bridge MMC and Traditional PSC for CHB

At first sight, the proposed PSC conspire for full-connect MMC are very comparable with the customary PSC plot for CHB, as they are both managing the full-connect SM and both equipped for expanding the equal switching frequency. Notwithstanding, there are checked contrasts between these two PSC plans, and it is basic to uncover them: (It is gathered that MMC and CHB have a similar number ($2N$) of full-connect SMs inside one phase. Thus, each arm of MMC contains N SMs.)

1) Carrier contrasts. For full-connect MMC, the transporters are conveyed equitably among the N SMs inside a similar arm (upper or lower), with the phase move of π/N . In the mean time, there ought to be an interleaved uprooting point between the upper-arm and lower-arm transporters, which should be planned painstakingly to enhance the output voltage (or the circulating current) harmonic components. Notwithstanding, since CHB does not have the dc terminal and accordingly has no circulating current, the customary PSC plan to CHB just needs to take

thought of the output voltage sounds, where the transporters are disseminated similarly among all the $2N$ SMs, with a phase move of $\pi/2N$.

2) Reference contrasts. It is anything but difficult to produce the references for CHB, as all the $2N$ SMs are regulated utilizing the same sinusoidal reference. Interestingly, as for MMC, the references ought to be grouped into the upper and the lower arm, and a $1/4$ dc voltage move ought to likewise be presented, as appeared in (40) and (41).

FUZZY LOGIC CONTROLLER

Fuzzy rationale is a type of numerous esteemed rationales in which reality estimations of variables might be any genuine number somewhere around 0 and 1. By differentiation, in Boolean rationale, reality estimations of variables may just be 0 or 1. Fuzzy rationale has been stretched out to handle the idea of halfway truth, where reality quality may extend between totally genuine and totally false. Besides, when etymological variables are utilized, these degrees might be overseen by particular capacities.

Normally fuzzy rationale control system is made from four noteworthy components exhibited on Figure fuzzification interface, fuzzy induction motor, fluffy principle grid and defuzzification interface. Every part alongside fundamental fuzzy rationale operations will be depicted in more detail below

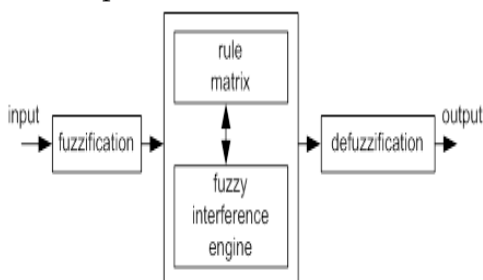


Fig:5 block diagram of fuzzy logic controller

The fuzzy rationale investigation and control strategies appeared in Figure 1 can be depicted as:

1. Receiving one or expansive number of estimations or other appraisal of conditions existing in some system that will be dissected or controlled.

2. Processing all got inputs as indicated by human based, fuzzy "assuming then" standards, which can be communicated in basic dialect words, and consolidated with conventional non-fuzzy preparing.

3. Averaging and weighting the outcomes from all the individual principles into one single output choice or sign which chooses what to do or advises a controlled system what to do. The outcome output sign is an exact defuzzified esteem. First of all, the different level of output (high speed, low speed etc.) of the platform is defined by specifying the membership functions for the fuzzy sets.

VI. CONCLUSION

This paper has modeling a hypothetical analysis of the PSC modulation for the MMC. Fundamental working standards of PSC utilized as a part of MMC and the relating capacitor voltage balancing technique are presented. The outstanding Fourier arrangement is used to measure the harmonic components of the output voltage and also circulating current. At that point, it is discovered that the harmonic extents of the output voltage and the circulating current are elements of the displacement angle between the upper and lower arms. In light of the analysis, the optimum displacement angle to limit the output voltage harmonics and to dispense with the exchanging harmonics of circulating current are identified, individually. Besides, harmonic qualities of the line-to-line voltage and the dc-link current are additionally created. Regarding MMC with full-connect SMs, an modulation of the PSC conspire is additionally proposed which can expand the proportional switching frequency and hence lessen the extent of required filters. The legitimacy of the numerical investigation and the proposed techniques are affirmed by tests in view of a three-phase MMC model and we can reach the inference that the PSC

balance is an adaptable and powerful PWM solution for MMCs.

VII. REFERENCES

- [1]. B. Bose, "Global energy scenario and impact of power electronics in 21st. century," *IEEE Trans. Ind. Electron.*, vol. 60, no. 7, pp. 2638-2651, Jul. 2013.
- [2]. I. Erlich, F. Shewarega, C. Feltes, F. W. Koch, and J. Fortmann, "Offshore wind power generation technologies," *Proc. IEEE*, vol. 101, no. 4, pp. 891-905, Apr. 2013.
- [3]. C. C. Davidson and G. De Preville, "The future of high power electronics in transmission and distribution power systems," presented at the 13th Eur. Conf. Power Electron. Appl. (EPE), Barcelona, Spain, Sep. 8-10, 2009.
- [4]. A. Lesnicar and R. Marquardt, "An innovative modular multilevel converter topology suitable for a wide power range," presented at the IEEE PowerTech Conf., vol. 3, Bologna, Italy, Jun. 23-26, 2003.
- [5]. H. Akagi, "Classification, terminology, and application of the modular multilevel cascade converter (MMCC)," *IEEE Trans. Power Electron.*, vol. 26, no. 11, pp. 3119-3130, Nov. 2011.
- [6]. R. Marquardt, "Modular multilevel converter: An universal concept for HVDC-networks and extended DC-bus-applications," presented at the Int. Power Electron. Conf., Sapporo, Japan, Jun. 2010.
- [7]. J. Glasdam, J. Hjerrild, L. H. Kocewiak, and C. L. Bak, "Review on multilevel voltage source converter based HVDC technologies for grid connection of large offshore wind farms," in *Proc. PowerCon.*, 2012, vol. 1, pp. 79-84.
- [8]. K. Friderich, "Modern HVDC PLUS application of VSC in modular multilevel converter topology," in *Proc. Int. Symp. Ind. Electron.*, Jul. 2010, pp. 3807-3810.
- [9]. K. Ilves, A. Antonopoulos, S. Norrga, and H.-P. Nee, "Steady-state analysis of interaction between harmonic components of arm and line quantities of modular multilevel converters," *IEEE Trans. Power Electron.*, vol. 27, no. 1, pp. 57-68, Jan. 2012.
- [10]. A. Antonopoulos, L. Angquist, and H.-P. Nee, "On dynamics and voltage control of the modular multilevel converter," in *Proc. 13th Eur. Conf. Power Electron. Appl. (EPE)*, Barcelona, Spain, Sep. 8-10, 2009.
- [11]. L. Angquist, A. Antonopoulos, D. Siemazko, K. Ilves, M. Vasiladiotis, and H.-P. Nee, "Open-loop control of modular multilevel converters using estimation of stored energy," *IEEE Trans. Ind. Appl.*, vol. 47, no. 6, pp. 2516-2524, Nov./Dec. 2011.
- [12]. L. Harnefors, A. Antonopoulos, S. Norrga, L. Angquist, and H.-P. Nee, "Dynamic analysis of modular multilevel converters," *IEEE Trans. Ind. Electron.*, vol. 60, no. 7, pp. 2526-2537, Jul. 2013.
- [13]. U. N. Gnanarathna, A. M. Gole, and R. P. Jayasinghe, "Efficient modeling of modular multilevel HVDC converters (MMC) on electromagnetic transient simulation programs," *IEEE Trans. Power Del.*, vol. 26, no. 1, pp. 316-324, Jan. 2011.
- [14]. M. Guan and Z. Xu, "Modeling and control of a modular multilevel converter-based HVDC system under unbalanced grid conditions," *IEEE Trans. Power Electron.*, vol. 2, no. 12, pp. 4858-4867, Dec. 2012.
- [15]. D. Pefitsis, G. Tolstoy, A. Antonopoulos, J. Rabkowski, J.-K. Lim, M. Bakowski, L. Angquist, and H.-P. Nee, "High-power modular multilevel converters with SiC JFETs," *IEEE Trans. Power Electron.*, vol. 27, no. 1, pp. 28-36, Jan. 2012.
- [16]. S. Rohner, S. Bernet, M. Hiller, and R. Sommer, "Modulation, losses, and semiconductor requirements of modular multilevel converters," *IEEE Trans. Ind. Electron.*, vol. 57, no. 8, pp. 2633-2642, Aug. 2010.
- [17]. J. Qin and M. Saeedifard, "Predictive control of a modular multilevel converter for a back-to-back HVDC system," *IEEE Trans. Power Del.*, vol. 27, no. 3, pp. 1538-1547, Jul. 2012.
- [18]. M. Hagiwara and H. Akagi, "Control and experiment of pulsewidth modulated modular multilevel converters," *IEEE Trans. Power Electron.*, vol. 24, no. 7, pp. 1737-1746, Jul. 2009.
- [19]. Q. Tu, Z. Xu, and L. Xu, "Reduced switching-frequency modulation and circulating current suppression for modular multilevel converters," *IEEE nTrans. Power Del.*, vol. 26, no. 3, pp. 2009-2017, Jul. 2011.
- [20]. M. Hagiwara and H. Akagi, "Control and analysis of the modular multilevel cascade converter based on double-star chopper-cells (MMCCDSCC)," *IEEE Trans. Power Electron.*, vol. 26, no. 6, pp. 1649-1658, Jun. 2011.